Cell

Schwann Cell Precursors from Nerve Innervation Are a Cellular Origin of Melanocytes in Skin

Igor Adameyko,[1,8] Francois Lallemend,[1,8] Jorge B. Aquino,[1,2] Jorge A. Pereira,[3] Piotr Topilko,[4] Thomas Müller,[5] Nicolas Fritz,[1] Anna Beljajeva,[6] Makoto Mochii,[7] Isabel Liste,[1] Dmitry Usoskin,[1] Ueli Suter,[3] Carmen Birchmeier,[5] and Patrik Ernfors[1,*]

[1]Unit of Molecular Neurobiology, Department of Medical Biochemistry and Biophysics, Karolinska Institute, 17177 Stockholm, Sweden
[2]Liver Unit, School of Medicine, Austral University, Avenida Presidente Perón 1500 (B1629ODT) Derqui-Pilar, Buenos Aires, Argentina
[3]Institute of Cell Biology, Department of Biology, ETH Zürich, CH-8093 Zürich, Switzerland
[4]Laboratoire de Génétique Moléculaire du Développement, Inserm 784, Ecole Normale Supérieure, 45 rue d'Ulm, 75230 Paris cedex 05, France
[5]Neuroscience Department, Max-Delbrück-Centrum for Molecular Medicine, Robert-Rössle-Strasse 10, 13125 Berlin, Germany
[6]Department of Cell and Molecular Biology, Medical Nobel Institute, Karolinska Institute, Stockholm, Sweden
[7]Department of Life Science, Graduate School of Life Science, University of Hyogo, 3-2-1 Kouto, Kamigori, Akou, Hyogo 678-1297, Japan
[8]These authors contributed equally to this work
*Correspondence: patrik.ernfors@ki.se
DOI 10.1016/j.cell.2009.07.049

SUMMARY

Current opinion holds that pigment cells, melanocytes, are derived from neural crest cells produced at the dorsal neural tube and that migrate under the epidermis to populate all parts of the skin. Here, we identify growing nerves projecting throughout the body as a stem/progenitor niche containing Schwann cell precursors (SCPs) from which large numbers of skin melanocytes originate. SCPs arise as a result of lack of neuronal specification by Hmx1 homeobox gene function in the neural crest ventral migratory pathway. Schwann cell and melanocyte development share signaling molecules with both the glial and melanocyte cell fates intimately linked to nerve contact and regulated in an opposing manner by Neuregulin and soluble signals including insulin-like growth factor and platelet-derived growth factor. These results reveal SCPs as a cellular origin of melanocytes, and have broad implications on the molecular mechanisms regulating skin pigmentation during development, in health and pigmentation disorders.

INTRODUCTION

Melanocytes, or pigment cells, represent a significant proportion of the cells in the adult epidermis, with about 800 cells/mm^3. Melanin, which is produced by melanocytes, is the main contributor to pigmentation and is packaged and delivered to keratinocytes by lysosome-like structures called melanosomes. The skin, as the main barrier to the external environment, relies on melanocytes to provide photoprotection and thermoregulation via the production of melanin.

The current view of how melanocytes populate the skin is that their precursors, the melanoblasts, arise from the neural crest (NC), which is induced by Bone morphogenic protein (BMP) and Wnt signals at the time of closing of the neural tube, and enter the ectoderm almost immediately, migrating in its vicinity following well defined routes (Dorris, 1938, 1939; DuShane, 1935; Rawles, 1947; Ris, 1941; Twitty, 1936). First, they migrate dorsolaterally between the dermamyotome and the overlaying ectoderm and then ventrally through the developing dermis to their eventual destination in the basal layer of the epidermis and the hair follicles (Erickson, 1993). This hypothesis accounts for that neural crest cells (NCCs) commit to a melanocyte fate already at the level of the neural tube, shortly after NC delamination. The origin and stereotypic migratory pathway of skin melanocytes have become widely accepted in the literature and are mainly supported by experiments using radioautographic or quail-into-chick transplantation systems, vital dye tracing in chick and mouse, and genetic targeting to express reporter markers under melanoblast- and melanocyte-specific protein promoters in mouse (Bronner and Cohen, 1979; Johnston, 1966; Le Douarin, 1973; Mackenzie et al., 1997; Rawles, 1947; Serbedzija et al., 1989, 1990; Weston, 1963). These studies describe the emergence of melanoblasts between the dermamyotome and ectoderm. However, the eventual migration within the prospective dermis to ventral body regions and limbs has not been fully addressed and it has been observed that melanoblasts appear precociously and localize at least to the limbs without an apparent dermal migration (Fox, 1949). The clonal expansion of founder melanoblasts, which mix and disperse only to a limited degree during migration under the epidermis, is thought to give rise to coat pigmentation (Mintz, 1967) and to underlie the observation of defined pigmentation patches appearing from individual melanoblasts (Huszar et al., 1991; Wilkie et al., 2002).

Early delaminating NCCs take the ventral pathway of migration and differentiate into neurons and Schwann cell precursors (SCPs). SCPs are defined as Sox10$^+$ NCC-derived cells tightly associated with neuronal projections during early stages of embryonic development that are able to migrate long distances along the nerves (Jessen and Mirsky, 2005). NCCs that acquire a melanoblast fate emerge lastly at the dorsal neural tube and migrate following a dorsolateral pathway. The difference in timing between these waves correlates with the period of conversion of the epithelial somite into the dermamyotome, and these spatial and temporal changes in the presence of instructive signals are believed to instruct the late NCCs to acquire a melanocyte fate. In chick and mouse, Wnt1 promotes melanoblast formation and reduces formation of neurons and glia via β-catenin (Dunn et al., 2000; Jin et al., 2001) in part by inducing the shared multipotent NCC/melanocyte SRY-related high-mobility-group domain transcription factor Sox10 (Aoki et al., 2003; Honore et al., 2003). As a central regulator of pigment cell development, microphthalmia-associated transcription factor (Mitf) determines a melanocyte fate of multipotent NCCs in part by its potent transcriptional and lineage-specific regulation of the three major pigment enzymes: tyrosinase, Tyrp1, and Dct as well as other pigmentation factors (Steingrimsson et al., 2004). In Zebrafish, the Wnt pathway also promotes a commitment to the melanocyte lineage by a direct transcriptional regulation of the Mitf gene (Dorsky et al., 2000). Consistent with a source of Wnt signals from the neural tube shortly after NC delamination, and hence the current view of the origin and migration of melanoblasts, the analysis of Mitf expressing cells has confirmed a commitment of NCCs at the dorsal neural tube and the presence of Mitf positive cells underneath the ectoderm at the level of the dermamyotome during development (Nakagawa and Takeichi, 1998).

In this study, we confirm the previously described source of skin melanocytes from the delaminating NCCs at the dorsal neural tube, and we provide evidence that large numbers of melanocytes are also produced from nerves innervating the skin. The cellular origin of these cells are Sox10$^+$/Krox20$^-$ SCPs of the trunk ventral migratory pathway. We show that myelinating Krox20$^+$ Schwann cells normally do not differentiate into melanocytes but retain the competence to do so. The SCP versus melanocyte fate in nerves is intimately linked to cellular contact with the nerve and depends on interactions with Neuregulins and their ErbB3 receptor, revealing a dual role for this signaling system in the developing nerve. In addition, insulin-like growth factor 1 (IGF1) and platelet-derived growth factor (PDGF) act in an opposing manner to Neuregulins promoting, in the later waves melanocyte differentiation, survival, and expansion from SCPs.

RESULTS

Melanocyte Development Is Associated with SCPs and Nerves

Melanoblasts are believed to follow a single highly stereotyped dorsolateral pathway from their origin in the dorsal neural tube to their final target, the skin. Consistent with this, Mitf$^+$/Sox10$^+$ melanoblasts were seen at the dorsal neural tube in the Hamburger Hamilton stage (HH) 22 in chick. Labeled cells were located in the trunk along the lateral edges of the embryo under the epidermis at the extent of the dermamyotome but were never located in the ventral body wall or the limbs (Figure 1A). Between HH24 and 27, these cells were reduced in number with the remaining few cells being located at dorsal aspects of the embryo (Figures 1H and 1L, arrowheads).

At late HH22, a second presence of Mitf$^+$/Sox10$^+$ melanoblasts spatiotemporally distinct from the previously described dorsolateral pathway was observed within the distal ventral ramus of the spinal nerve (Figures 1B, 1D, and 1E, indicated 2a). Weak levels of MITF expression appeared inside of Tuj1$^+$ nerve bundles colocalizing with Sox10$^+$ SCP nuclei while MITF expression was stronger in cells associated but not in direct contact with nerves, suggesting that melanocytes arise from Sox10$^+$ SCPs of the nerves (Figures 1C–1F). At HH24, an increased number of Mitf$^+$/Sox10$^+$ melanoblasts associated with ventral ramus nerves was observed (Figures 1H, 1J, and 1K). At this stage, when the dorsal ramus was not clearly established, the presence of a few Mitf$^+$/Sox10$^+$ melanoblasts located between the DRG, dermamyotome, and skin that were not in contact with nerves indicated that some Sox10$^+$ dorsal root ganglion "border cells" (Montelius et al., 2007) might migrate unguided by nerves through the dermamyotome to the lateral body wall, acquiring MITF expression on the way. Overall, this contribution appeared minor as at HH27-29, larger numbers of Mitf$^+$/Sox10$^+$ melanoblasts were observed along the newly formed dorsal rami nerves which innervate the skin and axial muscles of the dorsal and lateral trunk (Figures 1M, indicated 2b). At this stage, melanoblasts appeared in even greater number around the ventral spinal nerves as compared to HH24 (Figures 1L and 1N and Figure S1A available online). Quantification showed that while the first (dorsolateral) wave contributed with a majority of Mitf$^+$ cells at HH21-22, ventral ramus associated Mitf$^+$ cells increased with time (i.e., HH27-28; Figure 1G).

Chick embryos electroporated in the neural tube with a green fluorescent protein (GFP) expression construct for NCC tracing were used to address if melanoblasts produced from spinal nerves were NC-derived and whether they originated from SCPs associated with nerve fibers. At HH22, GFP$^+$ cells within the nerves were occasionally Sox10$^+$/Mitf$^+$ while GFP$^+$ cells that were very close (i.e., associated with), but not in direct contact with the nerve, were always Sox10$^+$/Mitf$^+$ (Figure 1I and inset). At HH24 and 27 most Sox10$^+$/Mitf$^+$/GFP$^+$ cells were associated with nerves extending toward the skin (Figures 1H and 1J–1M) with "hot spots" at distal ends of the dorsal and ventral ramus and brachial plexus, together with smaller nerve branches of limbs (Figures 1I–1M and S1A–S1D, summarized in 1N). Similar results were obtained in the mouse. At E10.5 the first wave (i.e., dorsolateral pathway) of Mitf$^+$/Sox10$^+$ melanoblasts was evident (Figure 1O). In the chick, a marked reduction in cells of the first wave was observed as described above, but in mouse at E11.5, the majority of melanoblasts in the dorsolateral aspect of the embryo was absent. At E12, a few Mitf$^+$/Sox10$^+$ melanoblasts were closely associated with cutaneously located spinal nerves of the dorsal rami (Figures 1Q and 1S) with increasing numbers at E13 (Figure 1R, summarized in S2A).

Quantification confirmed a reduction of melanoblasts from the first wave and a later increase now associated with nerves (Figure 1P). Nerve-associated Mitf$^+$ cells were confirmed to be

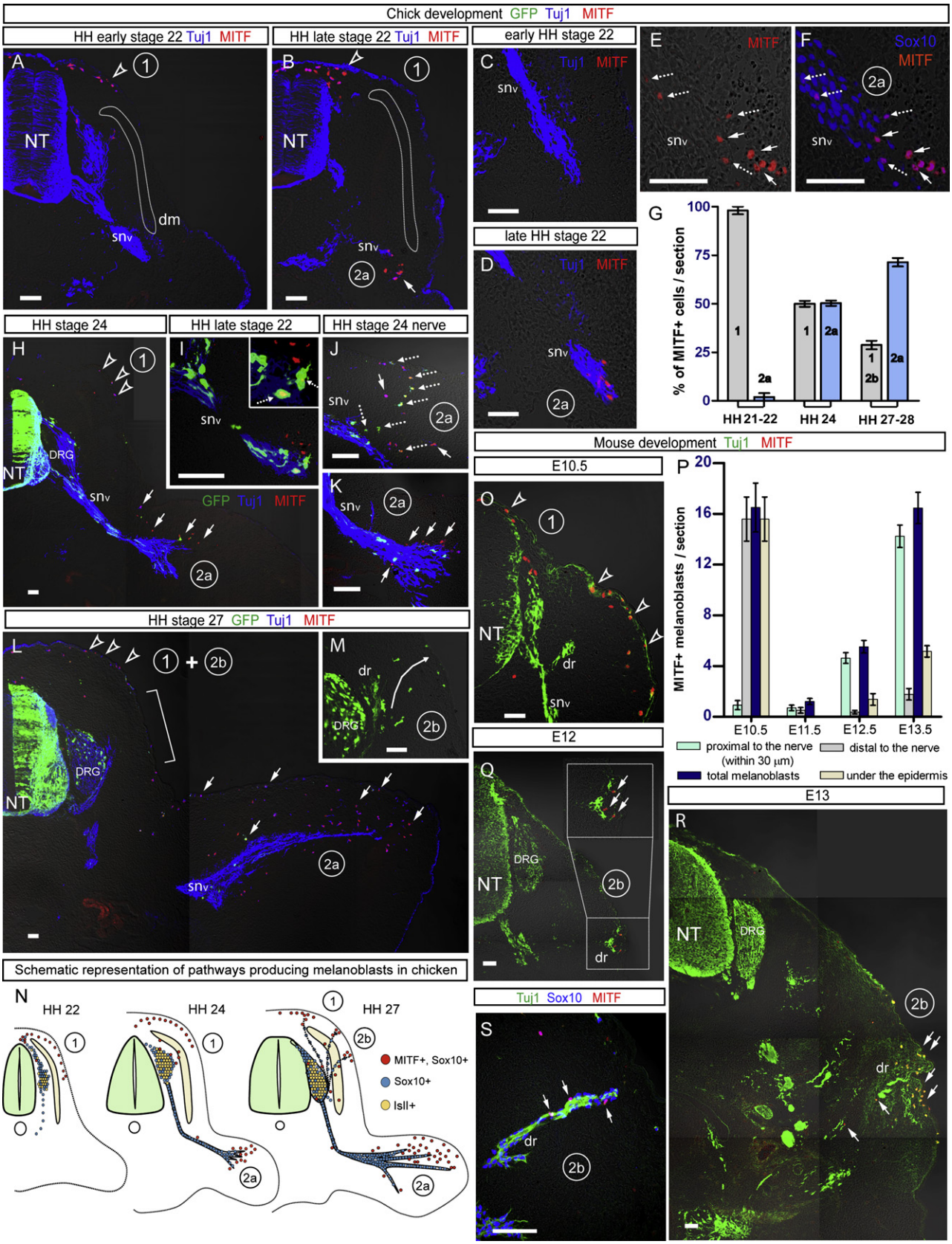
Chick development GFP Tuj1 MITF
HH early stage 22 Tuj1 MITF
HH late stage 22 Tuj1 MITF
early HH stage 22
late HH stage 22
A
B
C
D
E
F
G
NT
dm
snv
MITF
Sox10 MITF
Tuj1 MITF
% of MITF+ cells / section
HH 21-22
HH 24
HH 27-28
HH stage 24
HH late stage 22
HH stage 24 nerve
H
I
J
K
DRG
GFP Tuj1 MITF
HH stage 27 GFP Tuj1 MITF
L
M
Mouse development Tuj1 MITF
E10.5
E12
E13
O
P
Q
R
dr
MITF+ melanoblasts / section
E10.5
E11.5
E12.5
E13.5
proximal to the nerve (within 30 µm)
distal to the nerve
total melanoblasts
under the epidermis
Schematic representation of pathways producing melanoblasts in chicken
N
HH 22
HH 24
HH 27
MITF+, Sox10+
Sox10+
Isl1+
Tuj1 Sox10 MITF
S

melanoblasts by their coexpression in chick with melanosome matrix protein (MEBL-1), which specifically recognizes avian melanocytes and their precursors, and in mouse by the coexpression with the tyrosinase family member dopachrome tautomerase (DCT), a key enzyme involved in the synthesis of the melanin pigment (Figure S3) (Jessen and Mirsky, 2005). Combined, these results show that during development emergence of melanoblasts is closely associated with SCPs of nerves in temporospatially distinct locations from that previously described in the dorsolateral pathway.

Defined and Independent Contribution of Nerve-Derived Melanoblasts

We next directly addressed if melanoblasts associated with nerves are derived from cells within the nerves (i.e., SCPs). One hemisphere of the chick neural tube together with the adjacent DRGs was ablated at the forelimb bud level just after the first melanocyte wave ceased (HH22; Serbedzija et al., 1989) (Figures 2A–2D). Mitf$^+$ cells in the dorsolateral pathway were unaffected by the ablation immediately and 6 hr after surgery (Figures 2N, S4A, and S4B). The embryos were previously electroporated with GFP for cell lineage tracing and were analyzed at HH28 (Figures 2C–2H). On the experimental side, a reduced number of Mitf$^+$ melanoblasts was observed in the dorsal and lateral body wall (Figures 2E and F) and an even greater loss in the limb (Figures 2H, S4C, quantification 2O). This shows that melanocytes were reduced in numbers as a consequence of eliminating the ventral migratory pathway.

To exclude that later nerve-associated melanoblasts appearing in the limb were derived from migrating melanoblasts of the dorsolateral pathway, we next surgically unilaterally ablated the dorsal and lateral surface of the embryo at HH22, including the delaminated melanoblasts of the dorsolateral pathway, but leaving the neural tube, DRG and ventrally migrating SCPs intact (Figures 2I–2L and S5A). Ablation of the first (dorsolateral) wave of melanoblasts did not quantitatively affect numbers of melanoblasts in the limb bud (Figures 2M and 2O). The GFP NCC lineage tracing in such ablated animals provided evidence for NC-derived SCPs in the ventral pathway of NC migration as an origin of melanocytes in the chick (Figures 2M and S5).

Our data suggest that not only melanocytes in the limbs originate from SCPs migrating along nerves but also a large number of melanocytes in the dorsal and lateral body wall. These may emerge partially from Sox10$^+$ DRG border cells but most abundantly from SCPs migrating along the dorsal ramus of the spinal nerve. To confirm these migratory paths we performed slice cultures of HH24 and 27 chick embryos previously electroporated with GFP to trace NC-derived cells. NCCs occasionally cross the hemisphere and contribute with cells to the contralateral side and if electroporated at HH13 they often contribute with border cells around the DRG (Figure S6A). Slice cultures were first prepared from HH24 when the DRG has just coalesced and the dorsal ramus nerve was not formed. Already after 6 hr in vitro, border cells divided and started to migrate laterally, and within 18 hr, many of the cells had migrated through the dermamyotome apparently independent of nerves (Figures S6A–S6D). When cultures were instead prepared from HH27 embryos the dorsal ramus was clearly distinguishable and at this developmental stage the SCPs migrated along the dorsal ramus to the dermis/epidermis (Figures S6E–S6H). This identifies that large numbers of SCPs migrate along nerves toward the skin where some acquire a melanoblast fate.

PLP$^+$ SCPs: A Cellular Origin of Melanocytes in the Mouse

We used inducible, tissue-specific genetic tracing to address the cellular and molecular identity of the precursors of melanoblasts in the mouse. Transgenic mice expressing the improved tamoxifen (TM)-inducible Cre recombinase (CreERT2) under the proteolipid protein (PLP) promoter that is active specifically in SCPs and Schwann cells (Leone et al., 2003) were crossed to the Rosa26-YFP reporter mouse strain that contains a floxed stop cassette preventing YFP expression. In such mice, TM treatment results in the excision of the stop cassette leading to the permanent expression of YFP in SCPs and, hence, also in all cells derived from SCPs. Injection of TM at E16 (when formation of new melanocytes has ceased) and analysis of YFP expression at E17 revealed labeling of Schwann cells within cutaneous nerves but not in Mitf$^+$ melanocytes, confirming that the PLP-CreERT2 transgene is not active in melanocytes (0/218 Mitf$^+$ cells, n = 4 animals; Figure 3A). When administrating TM at E11 and analyzing embryos at E13, similar to the experimental conditions (see below), YFP expression in Mitf$^+$ melanoblasts of the dorsolateral migratory pathway at sacral levels of the embryo was not observed (0/48 Mitf$^+$ cells, n = 4 animals,

Figure 1. Association of Melanoblasts with Nerves in Chick and Mouse Development

(A–N) Chick development, transverse sections through the trunk. (A) Mitf$^+$ melanoblasts in location of dorsolateral pathway (first wave, indicated by digit #1) at HH22. (B) Spatially distinct Mitf$^+$ cells located at ventral spinal nerves a few hours later (indicated by digit #2a). (C and D) Mitf$^+$ melanoblasts within ventral spinal nerve at late HH22. (E and F) Weak Mitf expression colocalizes with Sox10$^+$ cells within nerves (dotted arrows) with increased intensity in cells distal to the nerve (solid arrows). (G) Quantification of Mitf$^+$ cells in indicated spatiotemporal locations (wave 1, dorsolateral pathway; 2a ventral spinal nerve; 2b dorsal spinal nerve; n = 4 animals/stage; error bars represent SEM). (H–K) GFP tracing of NCCs at HH22 and HH24 (Dotted arrows point at Mitf$^+$/GFP$^+$ cells traced in location of spinal nerve and skin). (L) GFP tracing at HH27. Note increased number of Mitf$^+$ cells in proximity to ventral spinal nerve. White bracket indicates a spatial gap between wave 1 and 2a melanoblasts. (M) GFP traced cells associated with the dorsal spinal rami (indicated by digit #2b). (N) Schematic spatiotemporal representation of Mitf$^+$ melanocyte in the chick. (A–M) Solid arrows identify Mitf$^+$ cells in location 2a and arrowheads in 1 and 2b.

(O–S) Mouse development, transverse sections through the trunk. (O) Mitf$^+$ melanoblasts in the dorsolateral pathway at E10.5. (P) Quantification of Mitf$^+$ cells associated with peripheral nerves (n = 4 animals/stage; error bars represent SEM). (Q and R) Labeling for Mitf$^+$ at E12-13. Note absence of cells in location of dorsolateral (first) wave and appearance of increasing numbers of labeled cells in proximity to dorsal rami nerves (solid arrows: 2b wave). (S) Mitf and Sox10 double stained cells within dorsal rami nerves, similar to chick.

Abbreviations are as follows: NT, neural tube; DRG, dorsal root ganglion; dm, dermamyotome; dr, dorsal ramus; snv, ventral branch of spinal nerve. The scale bars represent 50 μm.

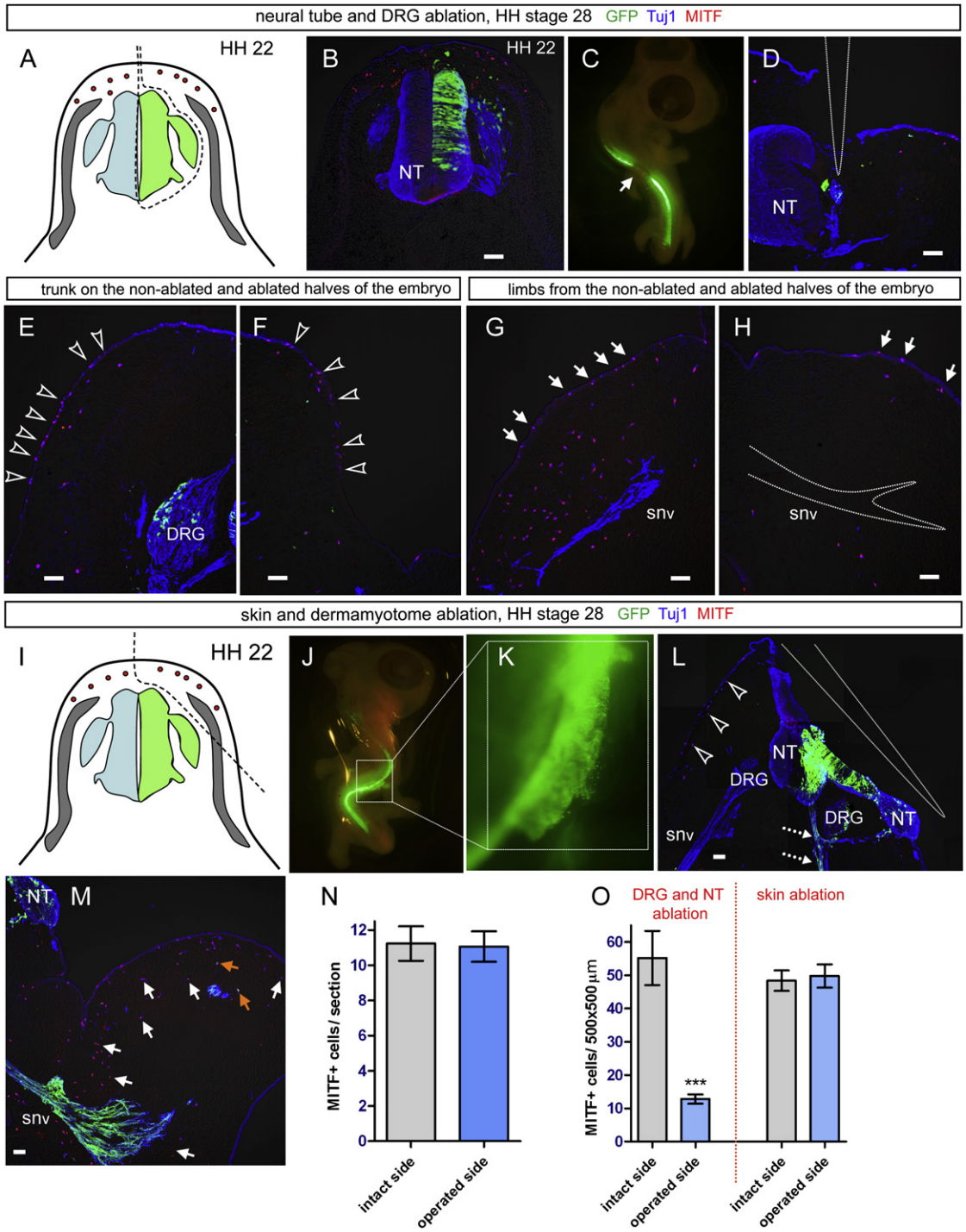

Figure 2. A Contribution of Melanoblasts from the Ventral Migratory Pathway

(A–H) Ablation of DRG and nerves, transverse sections through the trunk. (A) Schematic representation of the surgery at HH22 eliminating DRG and nerve-dependent pathways (green represents electroporated parts of the embryo, red circles represent melanoblasts). (B) Section of forelimb at stage when surgery was conducted. Note the presence of Mitf$^+$ melanocytes in the dorsolateral pathway. (C) Whole-embryo view 2 days after surgery (arrow indicating position of surgery). (D) Ablated side of the embryo showing near complete loss of GFP$^+$ nervous tissue. (E–H) Mitf$^+$ cells at trunk (E and F) and the dorsal limb level (G and H) of an operated embryo ([E and G] unoperated side; [F and H] operated side). Note loss of melanoblasts in (H), compared to (G), due to the lack of the ventral migratory pathway (dotted line marks the prospective position of the ventral spinal nerve).

(I–M) Ablation of skin and dermamyotome, transversal sections through the trunk. (I) Schematic representation of the surgery eliminating the dorsolateral melanoblast pathway at HH22. Whole (J), part (K), and section (L) view of operated embryo at time of analysis. (M) Mitf labeling of limb section on operated side. Note unaffected numbers of Mitf$^+$ cells. Orange arrows point at traced GFP$^+$ Smelanoblasts.

Figure S7A). PLP and Cre in situ hybridization confirmed their expression in ventral pathway including SCPs of nerves but not in the dorsolataral pathway or DCT$^+$ melanocytes at E10.5 (Figure S7). Furthermore, TM injection at E9.5, at the peak of NC delamination, and triple immunohistochemical staining for YFP, Cre and DCT at E10.5 confirmed recombination and Cre expression in cells of the ventral migratory pathway. However, a complete absence of Cre was observed in DCT$^+$ melanoblasts of the dorsolateral migratory pathway in the trunk (0/136 DCT$^+$ melanoblasts, n = 6 embryos, Figures 3B and 3C). In cranial nerves which are more advanced in development than the trunk and therefore could be analyzed in the E10.5 control embryos, Cre was specifically expressed in SCPs while genetically traced (YFP$^+$) Mitf$^+$ cells associated with nerves had downregulated Cre, showing that Cre expression is tightly associated with SCPs and is rapidly lost in cells detaching from the nerves (Figure 3D). Combined, these data confirm that PLP-Cre is not active in the NC dorsolateral pathway, melanoblasts or melanocytes. Examination of the dorsal ramus of the spinal nerve revealed a large number of Sox10$^+$/Mitf$^+$ cells expressing YFP often associated with cutaneous Tuj1$^+$ (βIII-tubulin$^+$) nerves (Figures 3E and 3F). The recombination frequency of Sox10$^+$ SCPs in the dorsal ramus was 63 ± 3% while the percentage of Sox10$^+$/Mitf$^+$ cells expressing YFP$^+$ was 61 ± 3.25% (Figure 3G), showing that the majority of Mitf$^+$ cells were derived from SCPs of the nerve. We next addressed if these melanoblasts contribute to melanocytes at postnatal stages. TM injection was performed at E11 and animals were collected at postnatal day (P) 11. Schwann cells of cutaneous nerves were YFP$^+$ (Figures S8C–S8E), consistent with their origin from SCPs. In addition, all hair follicles analyzed contained pigmented YFP$^+$ cells in skin of the trunk and extremities (200/200 follicles, n = 4 animals). Pigmented cells in hair follicles that were genetically traced (YFP$^+$) were double stained for DCT confirming that they were melanocytes. Similar results were obtained analyzing dermal melanocytes in both limbs and the trunk and quantification showed that 65.9 ± 3.1% and 58.6 ± 4.1% of the DCT$^+$ and pigmented cells in hair follicle and dermis, respectively, contained YFP (Figures 3H–3P). Pigmented and DCT$^+$ dermal melanocytes of glabrous skin (foot pad) were also YFP$^+$ (Figures S8A and S8B). These results confirm SCPs as an important cellular origin of pigmented dermal and hair follicle melanocytes and confirm that these cells populate cutaneous sites of the postnatal animal.

Hmx1 Regulates Neuronal versus Schwann Cell Precursor and Melanocyte Fates

Our previous results suggest that DRG border cells and SCPs along the nerves can be a cellular source of melanocyte precursors. Expression of a number of transcription factors (TFs) identified in the DRG (Marmigere et al., 2006; Gray et al., 2004) was analyzed.

The homeobox TF Hmx1 was absent in migrating NCCs at HH21 (Figure 4A) and increased as the NCCs coalesced into a DRG at HH24 (Figures 4B–4F). Hmx1 was exclusively localized to Islet-1$^+$ and mutually exclusive with Sox10$^+$ cells (marking neuroblasts and uncommitted NCC/glia progenitors, respectively; Figures 4C–4F) (Montelius et al., 2007), indicating that the onset of Hmx1 expression in the DRG coincides with the commitment to a neuronal fate. To assess the role of Hmx1 during DRG development, we developed two independent short interfering RNAs (siRNAs) against Hmx1. The efficiency of these siRNAs was tested in vitro and in vivo (Figures S9A–S9F). Control siRNA (scrambled) led to a contribution of electroporated cells that was similar to embryos only receiving GFP vector (Figure 4G). GFP$^+$ cells were seen at HH24 in nerves and the DRG, often colocalizing with Islet-1 (Figure 4G). Embryos receiving Hmx1 siRNAs displayed very few electroporated GFP$^+$ cells acquiring a neuronal fate in the DRG as seen by an almost complete complementary pattern of GFP$^+$ cells and neuronal markers Islet-1 and Tuj1. The electroporated cells were instead concentrated around the lateral border of the ganglion (i.e., DRG border cells, Figures 4H and 4I and S9G–S9H), some of them Mitf$^+$ melanoblasts and Sox10$^+$/Mitf$^+$/GFP$^+$ cells were observed between the DRG and the skin. At HH29 the skin showed a marked increase of Sox10$^+$/Mitf$^+$/GFP$^+$ melanoblasts compared to the control (scrambled siRNA) condition (Figures 4J–4M), which correlated with an increase in SCPs along dorsal rami spinal nerves in siHmx1 treated embryos (Figures 4J, 4K, S9I, and S9J). These findings show that a shift in the glia-neuronal balance can affect the amount of melanocyte precursors arising from late nerve-dependent pathways and that Hmx1 may act as a critical transcriptional switch between neuronal versus glia-melanocyte fates in the ventral NCC pathway.

Nerve-Schwann Cell Interactions during Melanoblast Development

In order to examine the role of nerve contact for differentiation of SCP-derived melanocytes, the spinal nerves proximal to the brachial plexus were transected on the GFP electroporated left side of HH27 chick embryos, and analyzed for Mitf expression at HH28 and 29. Compared to the unoperated contralateral forelimb, the operated limb exhibited a significant increase of Mitf$^+$ cells located in and around the region of the degenerating peripheral nerve at 12 and 24 hr after axotomization (Figures 5A–5E and S10). Often Mitf$^+$ cells were aligned with GFP traces of decaying electroporated nerve (Figure 5F). The increase of Mitf$^+$ cells was not caused by expansion of any already existing Mitf$^+$ cells since BrdU incorporation in such cells was not increased compared to control animals (Figure S11). These results demonstrate that maintenance of SCPs is nerve-dependent, as it has previously been shown (Jessen and Mirsky,

(A–M) Solid arrows mark nerve associated melanoblasts, arrowheads mark melanoblasts of dorsolateral pathway, dotted arrows point GFP$^+$ SCPs within nerve. Abbreviations are as follows: NT, neural tube; DRG, dorsal root ganglion. The scale bars represent 50 μm.

(N) Quantification of Mitf$^+$ cells at HH22 following ablation of DRG and nerves. Note that ablation does not affect numbers of Mitf$^+$ cells in dorsolateral pathway (n = 4; error bars represent SEM).

(O) Quantification of Mitf$^+$ cells in limbs from intact and operated sides of both ablation studies (n = 4 animals; error bars represent SEM; Students t test ***$p < 0.001$).

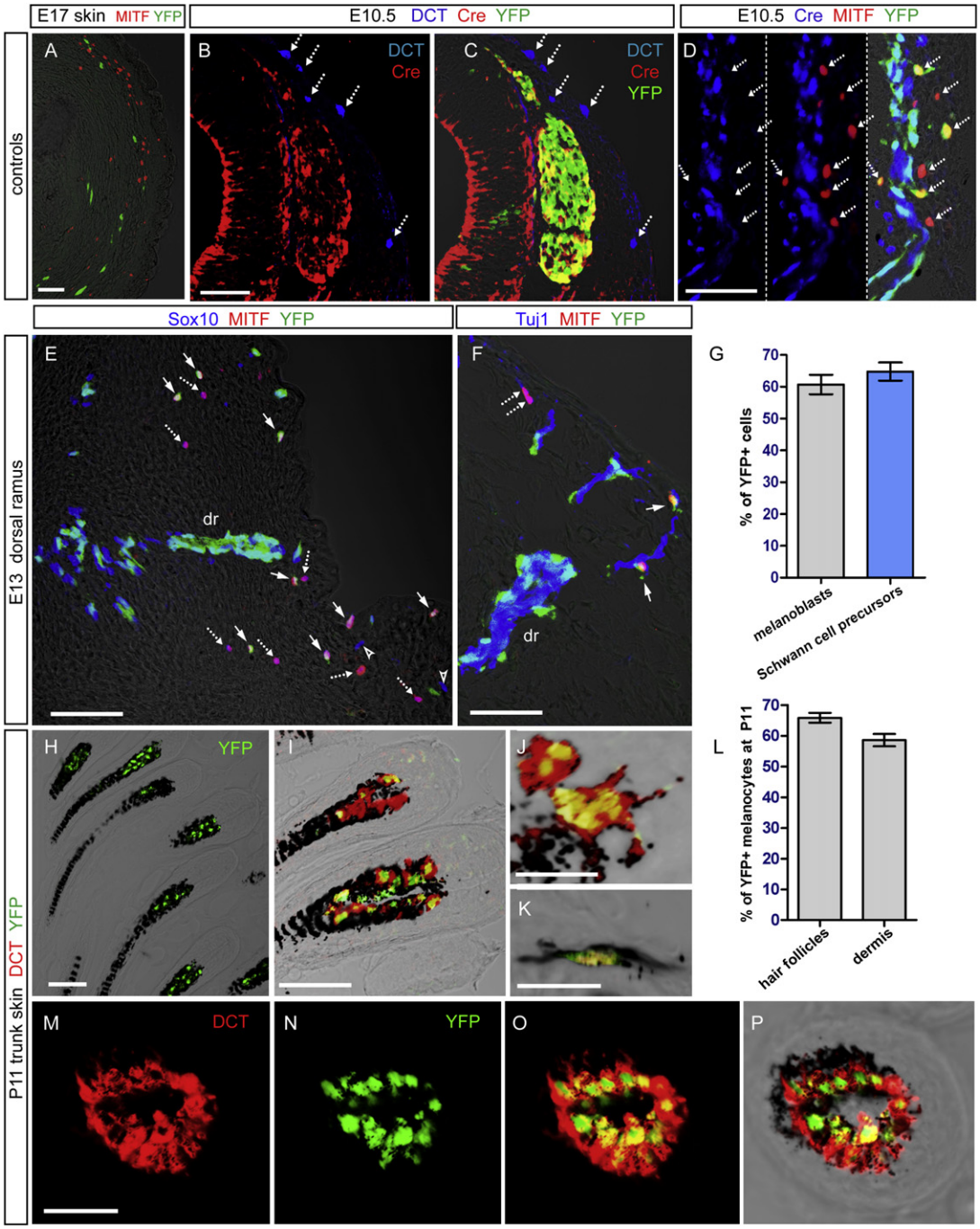

Figure 3. Genetic Tracing with PLP-CreERT2 Mice Confirms SCPs-Derived Origin of Embryonic and Adult Melanocytes in Mice

(A–D) Transversal section of genetic tracing controls. (A) Mitf labeling of E17 embryo 24 hr after tamoxifen administration. Note that Mitf$^+$ skin melanocytes do not express YFP while Schwann cells of cutanous nerves are positive. (B–D) E10.5 embryo injected with tamoxifen at E9.5 and stained for DCT or Mitf and Cre. Note expression of Cre and YFP (recombination) in the ventral pathway (B and C) and in SCPs (D), while Mitf$^+$ and DCT$^+$ melanoblasts are negative (dotted arrows).

(E–G) Genetic tracing of embryonic melanocytes by tamoxifen administration at E11 and analysis at E13. (E and F) Staining for YFP, Mitf and Sox10 or Tuj1 reveals recombination in SCPs and traced melanoblasts associated with Tuj1$^+$ nerves and dermis (Mitf$^+$ cells with punctuated arrows, and Mitf$^+$/YFP$^+$ solid arrows). (G) Quantification of YFP$^+$ cells among Sox10$^+$ SCPs and MITF$^+$ melanoblasts. Note that these numbers represent recombination frequency in nerve and the proportion of nerve-derived melanoblasts (n = 4 animals).

(H–P) Genetic tracing of postnatal melanocytes by tamoxifen administration at E11 and analysis at P11. Longitudinal (H and I) and transversal (M–P) sections of hair follicles traced with YFP and stained for DCT, as indicated. (J and K) High magnification of SCP traced (YFP$^+$) pigmented, DCT$^+$ pigmented hair follicle (J) and

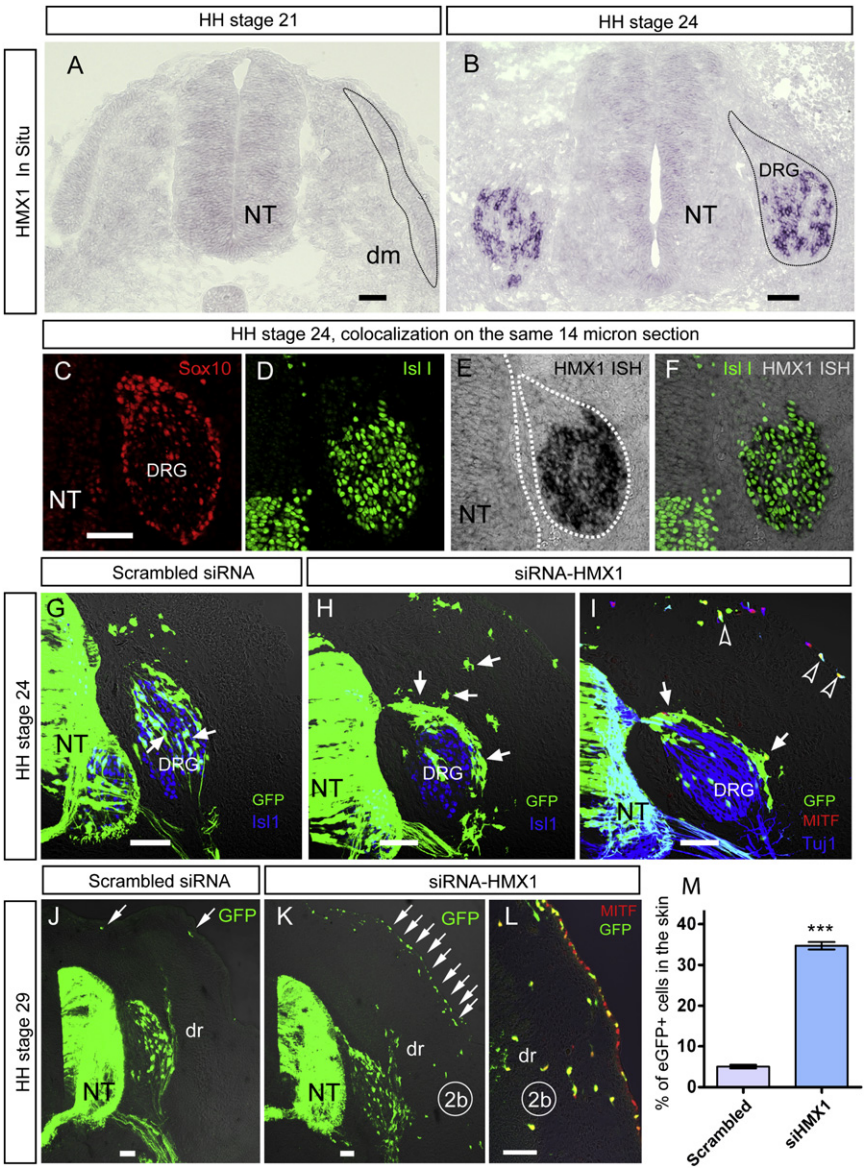

Figure 4. Hmx1 Expression Defines the Balance between Neurogenic and Glia-Melanocytic Fates in the Developing Dorsal Root Ganglion

(A and B) Transverse sections of HH21 (A) and HH24 (B) embryos hybridized with an Hmx1 antisense riboprobe. Note the detection of Hmx1 mRNA at the time of DRG condensation (illustrated at HH24) but not during NCC migration (HH21).

(C–F) HH24 forelimb DRG section triple stained for Hmx1 mRNA (Hmx1 ISH), Sox10, and Isl1. Note that Hmx1 colocalized with the neuronal marker.

(G–I) Hmx1 siRNA knockdown experiments at HH24. Note in experimental animals concentration of siRNA receiving (GFP^+) cells at border of the DRG, some expressing Mitf ([H and I] arrowheads mark dorsolateral melanoblasts).

(J–L) Hmx1 siRNA knockdown experiments at HH29. Note marked increase of siRNA receiving (GFP^+) cells in skin and which double stain for Mitf. (K and L) Digit 2b denotes dorsal rami associated cells.

(M) Quantification of percent of GFP^+ cells located in the skin at HH29 ($n = 6$ animals, $p < 0.001$; error bars represent SEM; Students t test ***$p < 0.001$).

Abbreviations are as follows: NT, neural tube; DRG, dorsal root ganglion; dm, dermamyotome; dr, dorsal ramus. The scale bars represent 50 μm.

2005), and that in the absence of signals provided by the nerve some SCPs instead acquire a melanocyte fate. This opens for that a competition of rapidly expanding numbers of SCPs for nerve contact may be a participating mechanism during the recruitment of melanoblasts populating the skin from nerves innervating the embryonic body.

Competence of Myelinating Schwann Cells to Generate Pigmented Cells in the Adult

The transcriptional factor Krox20/Egr2, that starts expression at E16 in mouse nerves, is critical for the differentiation of immature Schwann cells into myelinating Schwann cells (Topilko et al., 1994) and acts together with Sox10 to regulate myelin gene transcription (Steingrimsson et al., 2004). We addressed if nerve-derived melanocytes arise from SCPs prior to their specification to promyelinating and myelinating Schwann cells. Mice expressing a knock-in allele for the Cre recombinase in the Krox20 locus ($Krox20^{Cre/+}$) (Voiculescu et al., 2000) were combined with the Rosa26-YFP reporter strain for genetic tracing. YFP labeled cells were found in nerves of the adult mouse in close association with $neurofilament^+$ axons (Figure 6A), consistent with its expression in myelinating Schwann cells, as well as in hair follicles and epidermis (Figure 6B), as previously described (Gambardella et al., 2000). YFP was not observed in melanocytes of hair follicles and in melanocytes of the skin of the adult mouse (Figures 6B and 6C), showing that nerve-derived melanocytes do not differentiate during normal development from promyelinating and myelinating Schwann cells.

Our previous data showed a strong correlation between nerves and Schwann cell phenotype indicating that those cells staying in contact with nerves retain a SCP state and eventually differentiate into Schwann cells while cells detaching from the nerve acquire MITF expression. This raised the issue if

dermal (K) melanocytes. (L) Quantification of percent of melanocytes containing YFP in hair follicles and dermis at P11 ($n = 4$ animals). Note that the number is similar to the recombination frequency in SCPs.

Abbreviations are as follows: NT, neural tube ; NCC, neural crest cells ; dr, dorsal ramus. The scale bars represent 50 μm and 20 μm (J and K).

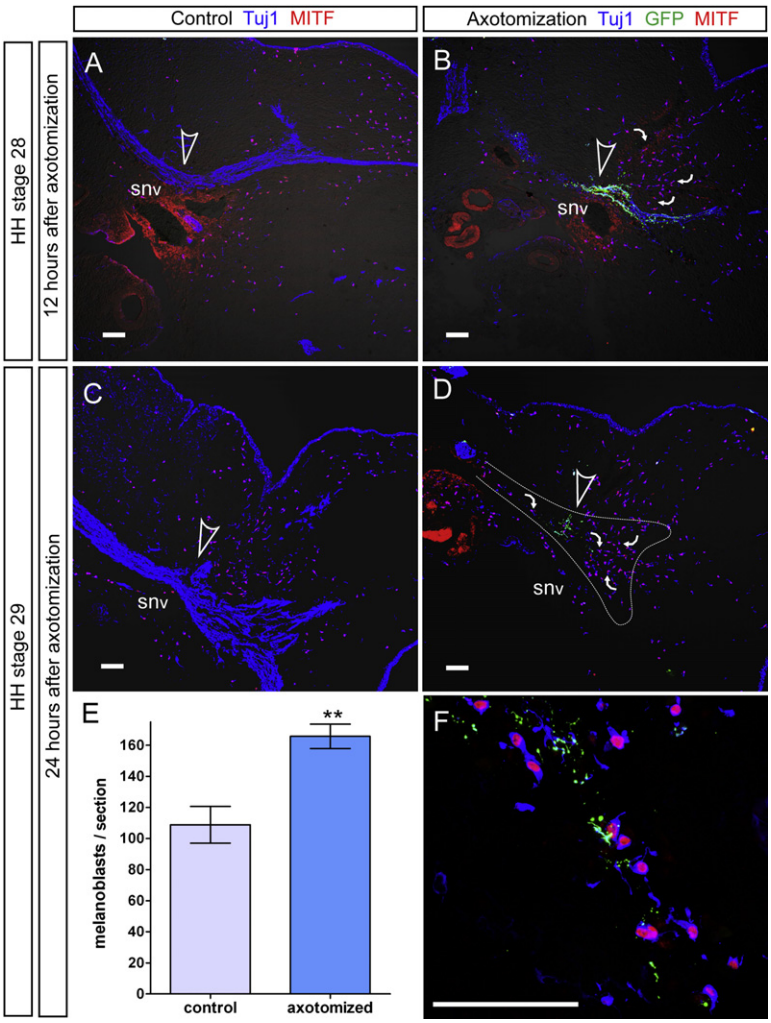

Figure 5. Excessive Melanocyte Numbers upon Loss of SCP-Nerve Contact

(A–D and F) Microsurgery-induced nerve axotomization at HH27 analyzed in transverse sections of HH28 (A and B) and HH29 (C, D, and F) embryos at the forelimb level, on the unoperated (A and C) and operated (B, D, and F) sides. Note the appearance of Mitf$^+$ melanoblasts at the place of the degenerating nerve 12 (B) and 24 hr (D and F) after surgery. Remnants of nerves seen by GFP fluorescence (arrowheads mark the equivalent positions on the control and operated sides, curved arrows Mitf$^+$ cells).

(E) Quantification of melanoblasts inside of the limb on sections after microsurgery-induced nerve axotomization (n = 4 animals; error bars represent SEM; Students t test $^{**}p < 0.01$).

(F) Axotomized spinal nerve at high magnification of a GFP-traced chick embryo. Note Mitf$^+$ cells along the decaying ventral spinal nerve (residual GFP).

myelinating Schwann cells could have the potential to differentiate into melanocytes if nerve contact is perturbed. We therefore addressed whether Krox20$^+$ promyelinating and myelinating Schwann cells retain the competence to differentiate into melanocytes. We examined this by surgically cutting a 5 mm piece of the sciatic nerve, leaving the transected piece of nerve in position by sutures to connective tissue of the underlying muscle (Rizvi, et al., 2002). Eighty days later, clusters of highly pigmented cells around muscles extended for more than 1 cm around the nerve fragment in all animals (n = 8, Figures 6D–6G). This massive hyperpigmentation was also observed on the ventral portion of the dermis (Figures 6H and 6I) with pigmented cells occasionally located also within muscles (Figures 6J and 6K). A large number of pigmented melanocytes were YFP$^+$ around and within muscles (Figure 6K), in the dermis (Figure 6L) and within and around remnants of the denervated sciatic nerve fragment (Figures 6M–6O). These results suggest that during development the onset of Krox20 expression defines a restriction in fate that normally precludes their differentiation into pigmented cells, but that these cells remain competent to form pigmented cells if challenged with a new microenvironment resulting from a loss of nerve contact.

ErbB3 Signaling between Nerve and Schwann Cell Precursors Balance Glial versus Melanocyte Fates

NCCs which migrate along nerves and eventually adopt a Schwann cell fate rely on axonal signals for survival, proliferation and differentiation. A neuronally-derived signal regulating survival and proliferation is Neuregulin-1 (NRG1) (Lemke and Brockes, 1984), also named glial growth factor, Heregulin or Neu differentiation factor, and that signals through the receptor tyrosine kinase ErbB2 and ErbB3 heterodimer complex expressed by Schwann cells. NRG1 appeared as a possible signaling molecule regulating glial versus melanocyte fates because it is produced in sensory and motor neurons as a molecule inserted into the axonal membranes. We examined a possible role for NRG1 signaling in the formation of melanocytes during development in erbB3$^{-/-}$ mice (Riethmacher et al., 1997). The dorsolateral wave of Mitf$^+$ melanoblasts appearing close to the neural tube was unaffected in erbB3$^{-/-}$ mice at E10 (Figures 7A, 7B, and 7E) while increased number of melanoblasts was observed around distal ends of dorsal spinal nerves at E12 (Figures 7C and 7D) and quantification confirmed an increase of Mitf$^+$ cells to 178% that of control mice (Figure 7E), despite an overall reduction of SCPs along nerves (Figure S12). Combined, our data show that Neuregulin signaling regulates not only survival and proliferation of SCPs along nerves during development, but it also participates in the decision between Schwann cell versus melanoblast differentiation.

Soluble Signals Regulating Melanocyte Development

Several soluble signals have been proposed to regulate the proliferation and migration of melanocytes (Thomas and Erickson, 2008). Development of melanocytes in different time and location from that previously thought open for soluble signals

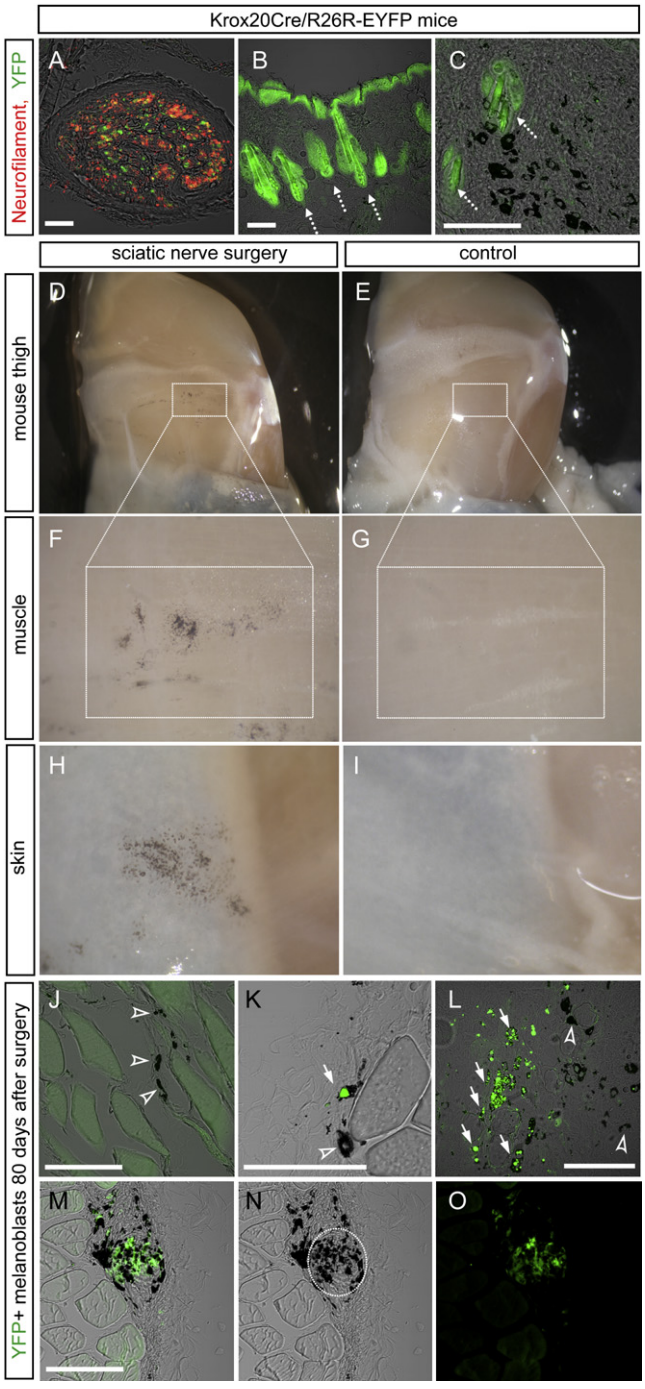

Figure 6. Mature Schwann Cells in the Adult Retain the Potential to Differentiate into Melanocytes

(A–C) Tracing of cell progenies using a Krox20-Cre locus crossed to a YFP reporter strain. (A) YFP in myelinating Schwann cells on a transverse section of the sciatic nerve. (B) YFP in the hair shafts and epidermis. (C) Pigmented cells in the skin were not positive for YFP. (B–C) Dotted arrows mark GFP$^+$ hair follicles.

(D–I) Sciatic nerve surgery experiment. Pigmented melanocytes was found at 80 days after sciatic nerve surgery inside of the thigh (D), connective tissue (F), and skin (H). (E, G, and I) Pigmented cells were not found in the contralateral control thigh.

(J–O) YFP tracing of cell progenies using a Krox20-Cre activating strain following sciatic nerve surgery. Note YFP$^+$ melanocytes between muscle fibers (J and K), connective tissue and dermis (L), and in the degenerated nerve stump of sciatic nerve (M–O). Dotted circle outlines the degenerated distal nerve stump. Solid arrows mark YFP$^+$ melanocytes, arrowheads point YFP$^-$ melanocytes.

The scale bars represent 50 μm.

partly different from those previously described. Two different in vitro assays were developed to address the role of previously unidentified soluble signals. In the first assay progenitor cells of HH29 DRG can stay in contact with axons and survive independent of signals added to the medium and could therefore be used to identify instructive and proliferative signals (Figures S13A–S13G). Low numbers of Mitf$^+$ melanocytes were seen in control cultures and NRG1 led to their reduction, consistent with our previous in vivo data. Insulin-like growth factor 1 (IGF1) and platelet-derived growth factor (PDGF) which are produced in the developing nerves (Meier et al., 1999) in addition to the previously characterized hepatocyte growth factor (HGF), significantly increased Mitf$^+$ cells. In a combination of NRG1 and IGF1, the latter could efficiently compete with NRG1, which led to a presence of significant amounts of melanoblasts (Figures S13F and S13G).

In the second assay, pieces of the limb nerves containing SCPs were dissected out from HH29 chick embryos and cultured for 5 days. Under neutral medium conditions a near complete death of all SCPs allowed us to assay for survival effects (Figures S13H–S13L). NRG1 led to marked cell survival but only a few Mitf$^+$ melanocytes (Figures S13J and S13L). IGF1 led to significant cell survival and development of numerous Mitf$^+$ melanocytes and was found to partially compete with NRG1 signaling (Figures S13I, S13K, and S13L), while PDGF supported cell survival inefficiently and cultures displayed only a moderate increase in Mitf$^+$ cells (data not shown). These results suggest that the Schwann cell produced factors IGF1 and PDGF may act in an opposing manner to NRG1 during recruitment of melanoblasts from nerves in the developing embryo.

DISCUSSION

It has been widely accepted that during development NCCs delaminating from the neural tube acquire a melanocyte fate, migrate dorsolaterally to populate the epidermis and massively expand in numbers making up as much as 5%–10% of all cells in the epidermis of the adult. We now provide evidence suggesting that NCCs migrating in the ventral pathway, which previously were considered to contribute only to glia and neurons of the peripheral nervous system, are also a source of melanocytes.

Nerve-Derived Schwann Cell Precursors as a Cellular Source of Skin Melanocytes

Several independent experiments confirm SCPs along nerves as a cellular source of melanocytes. Immunohistochemical analysis identified melanoblasts associated with nerves temporospatially distinct from the dorsolateral pathway. Consistently, cell tracing in the chick showed that GFP$^+$ traced SCPs along nerves acquire Mitf and MEBL expression. Ablation experiments confirmed that

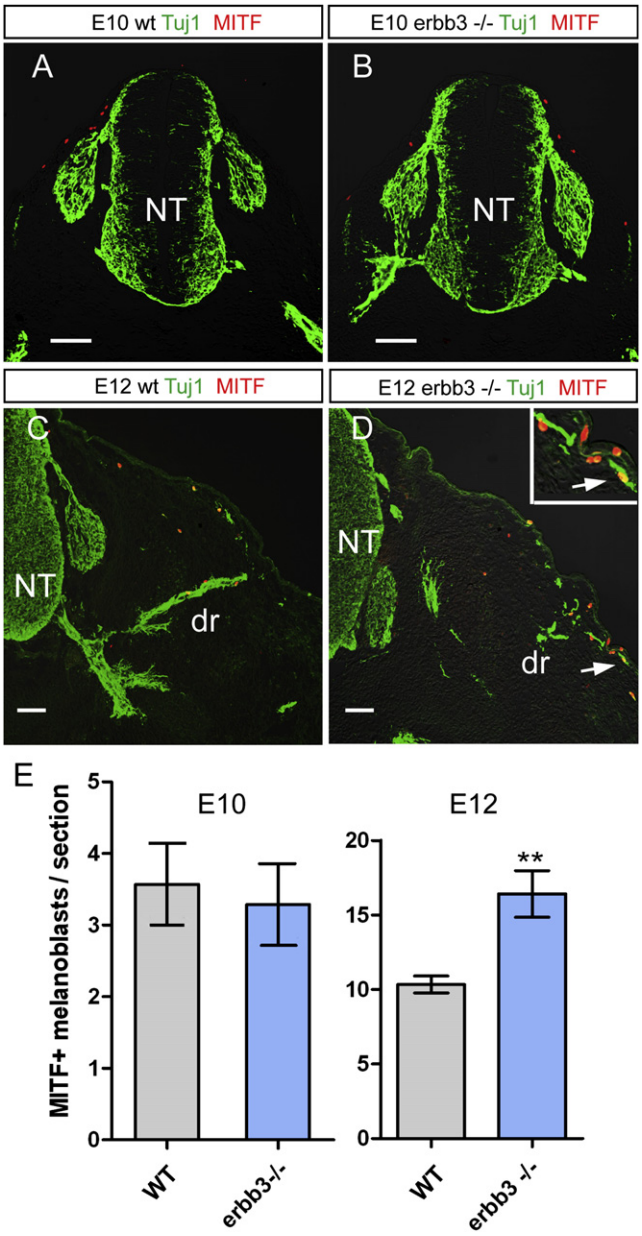

Figure 7. Regulation of SCP versus Melanocyte Fate by Neuregulin Signaling

(A–E) Melanocyte development in erbB3$^{-/-}$ and control mice. (A–D) Mitf and Tuj1 labeling of wild-type and erbB3$^{-/-}$ mice at E10 (A and B) and E12 (C and D). Arrow in the inset (D) points at melanoblast associated to the nerve fiber. (E) Quantification of Mitf^{+} melanoblast numbers in control and erbB3$^{-/-}$ embryos at E10 and E12 (n = 4 animals/group; error bars represent SEM; Students t test **p < 0.01,). Abbreviations are as follows: DRG, dorsal root ganglion; dr, dorsal ramus; NT, neural tube. The scale bars represent 50 μm.

the dorsolateral pathway did not affect GFP cell tracing of ventral pathway-derived melanocyte numbers while removal of neural tube and DRG resulted in greatly diminished numbers identifying SCPs as a cellular origin of melanoblasts in the chick. Some residual nerves were left in the limbs of ablated embryos which could be the source of the few remaining melanoblasts found in this location. SCPs as an origin of melanocytes were inferred from axotomization experiments both during development and in the adult in which loss of nerve contact lead to Mitf expression, consistent with our analysis of erbB3$^{-/-}$ mice also showing increased melanoblast numbers. Further corroboration is data showing that the homeobox transcription factor Hmx1, expressed only in neuronally committed cells but not in melanocytes, is required for neurogenesis and in its absence, increased numbers of non-neuronal progenies appear. Such increases resulted in marked elevations of melanocyte numbers in the skin. We used PLP-CreERT2 mice to genetically trace the progeny of PLP^{+} SCPs unequivocally identifying SCPs as a cellular origin of melanocytes during mouse development. This data also shows that DCT^{+}/Mitf^{+} mature pigmented melanocytes derived from SCPs appear at cutaneous sites in the postnatal animal. Combined all of these results together with time-lapse slice culture experiments corroborate our conclusion that SCPs along nerves innervating cutaneous tissues are an origin of melanocytes.

Our findings agree with, and may explain, some previous results. In contrast to Mintz's conjecture that a few founder melanoblasts gives rise to coat pigmentation (Mintz, 1967), more recent data show that there is a large number of melanoblast progenitors (Wilkie et al., 2002). Furthermore, when single NCCs were labeled by genetics, melanocytes coming from a single originating cell were located in patches in the skin intermingled with unlabeled cells. This shows that the progenitors disperse and mix but populate the skin in a defined patch (Huszar et al., 1991; Wilkie et al., 2002). It is conceivable that melanocytes arising from SCPs in cutaneous nerves could explain the observed patches of pigmentation which forms when individual labeled NCCs are studied. This phenotype could appear if cell division of rapidly migrating NCCs is limited and expansion of SCP and melanoblast numbers largely takes place within and around nerves terminating in specific cutaneous locations.

How Is Hmx1 Regulating Neuronal versus Melanocyte Cell Fates in the Ventral Migratory Pathway?

A melanoblast fate has been intimately linked with the timing of NC delamination. The NCCs migrate in chain-like structures with sympathetic neurons forming first, DRG neurons later and glial cells throughout this period while melanocytes are born from the last NCCs delaminating from the neural tube. The commitment of NCCs to a neuronal fate takes largely place within the coalescing ganglion where Neurogenins (Ngn1 and Ngn2) bias while Isl1 and FoxS1 marks a commitment to a sensory and neuronal fate, respectively (Zirlinger et al., 2002; Marmigere and Ernfors, 2007; Montelius et al., 2007). Those cells failing to initiate neurogenesis remain transiently as Sox10^{+} progenitors and are largely localized to the border of the ganglion, hence termed DRG border cells (Montelius et al., 2007). How does expression of Hmx1 fit into neurogenesis in the DRG and with the decision between a neuronal versus Sox10^{+} progenitor cell fate? We find that Hmx1 is not expressed in the migrating NCCs but is turned on within the DRG, coinciding with Islet-1 expression and that elimination of its expression using RNAi leads to near complete loss of neurogenesis. Instead, the cells remain as Sox10^{+} cells located around the lateral surface of

the DRG and shortly thereafter many acquire Mitf expression. The results imply Hmx1 as critical for decisions between neuronal and non-neuronal fates and also raise the possibility that it could repress the melanocyte fate and therefore in its absence, the cells in our experiments acquire a melanocyte fate. Although we can not exclude this possibility, it seems more likely that the melanocyte fate is secondary to the failure in neurogenesis. Differentiation of border cells into melanocytes could either be a consequence of instructive signals imposing this fate on the multipotent Sox10^{+} border cells or alternatively a default differentiation in the absence of instructive signals for other fates.

In invertebrate chordates, the ascidian urochordate *Ecteinascidia turbinate*, NC-like cells differentiate only into pigment cells. This opens for that evolution of NCCs begins with the generation of pigment cells and have gained additional functions to generate the full repertoire of cell types of the vertebrate NC lineage (Jeffery et al., 2004). This would imply that within NCCs, the melanocyte lineage is a default fate and the diversity of cell types produced in vertebrates is a consequence of acquirement of new coordinated signals maintaining their multipotency and instructing their differentiation into different cell types.

The Multipotent Schwann Cell Precursor

Early embryonic nerves are exclusively built from axon bundles and NC-derived cells. The NC-derived cells are intimately associated with the nascent nerves and start migrating their way through the body tissue along the nerves to reach distant targets. Once NCCs associate with axons of nascent nerves, they are considered as SCPs and express markers such as cadherin 19, ErbB3, protein 0 (P0), PLP and display a different responsiveness to survival factors compared with NCCs (Jessen and Mirsky, 2005). We find that this population of cells may also be the source of many melanocytes in the skin, suggesting that these cells share characteristics with multipotent stem cells. Hence, the growing nerves might be considered as stem/progenitor cell niches from which via inductive recruitment diverse cell types could be generated. We identify melanocytes as one such cell type, but the NC contributes with numerous cell types to a large number of tissues during embryogenesis. Future studies will have to address the role of the nerve SCPs as a cellular source for differentiated cell types in other tissues and organs.

The competence of Krox20^{+} myelinating Schwann cells derived from the deafferented adult nerves to differentiate into melanocytes in our experiments is likely a consequence of that cessation of proliferation in mature myelinating Schwann cells is reversible, as these cells can de-differentiate and re-enter the cell cycle upon nerve injury (Stewart et al., 1993; Dupin et al., 2003). A developmental origin of melanocytes from SCPs, a competence of Krox20^{+} Schwann cells and possibly of undifferentiated SCPs that could remain in the adult to generate melanocytes, may open insights in the numerous observed hypo- and hyper-pigmentation disorders caused by changes in the number of melanocytes, in mechanisms of re-pigmentation and in the association between neurological disorders and changes in skin pigmentation. For instance, neurofibromatosis type 1 patients which develop peripheral nerve tumors consisting mainly of Schwann cells and nerve sheath tumors also show skin hyperpigmentation (Fetsch et al., 2000; Weinreb et al., 2007). Recently, genotoxic stress was shown to result in melanocyte stem cell (MSC) depletion and irreversible hair graying due to their unscheduled differentiation (Inomata et al., 2009). The role of SCPs in the formation of new melanocytes in the adult, their role during age-related hair graying and the impact of genotoxic stress on a putative contribution of melanocytes from SCPs in the adult remains to be determined.

Nerve-SCP Interactions and Soluble Signals Regulating Melanocyte Development

Our results suggest that melanocyte development shares several signaling molecules with Schwann cell development. NRG1 plays an important role as an axonal signal for survival and proliferation of SCPs (Jessen and Mirsky, 2005). NRG1 is evidently not only a survival and proliferation signal for SCPs, given that the direct contact between the nerve and SCPs that is a prerequisite for Neuregulin signaling in SCPs, appears to suppress a melanocyte fate. In erbB3$^{-/-}$ mice we observed a significant increase of melanoblasts in and around the developing nerves despite significant loss of SCPs. Further, in DRG cultures containing border cells and in SCP cultures, NRG1 efficiently suppressed melanocyte differentiation.

The dependence on NRG1 for cell survival of SCPs ends with the transition to immature Schwann cells at which time the Schwann cells produce and respond to the survival factors IGF1 and PDGF (Meier et al., 1999). Our results show that IGF1 and PDGF efficiently instruct a differentiation of SCPs along a melanocyte cell lineage and that IGF/PDGF signaling and Neuregulin signaling may compete with opposing results. Hence, it is conceivable that as glial precursors expand in numbers Neuregulin signaling becomes limiting due to competition for nerve contact. In parallel, as increasing amounts of SCPs differentiate into immature Schwann cells and levels of IGF1/PDGF increase, the balance of Neuregulin and IGF1/PDGF signaling is shifted in favor of melanocyte differentiation. A similar mechanism might occur in the adult during nerve damage which leads to increased expression of IGF1/PDGF (Meier et al., 1999) and a reduced or complete loss of the nerve-derived Neuregulin signaling.

EXPERIMENTAL PROCEDURES

Mouse Strains

The generation and characterization of PLP-CreERT2, erbB3$^{-/-}$ and Egr2$^{Cre/+}$ R26R-YFP (Krox20^{YFP}) mice have been previously described (Leone et al., 2003; Maro et al., 2004; Riethmacher et al., 1997).

In Situ Hybridization and Immunohistochemistry

Embryos were fixed in 4% paraformaldehyde/PBS, cryoprotected and sectioned at 14 μm thickness. In situ hybridization experiments were performed as previously described (Marmigere et al., 2006). Detailed protocols and information on antibodies, immunohistochemistry and ISH are provided as Supplemental Data.

In Ovo Transfection

In ovo microinjections and electroporation of plasmids and siRNAs were carried out as previously described (Marmigere et al., 2006). siRNA sequences are detailed in the Supplemental Data.

BrdU Administration In Ovo

BrdU in a concentration of 100 μM was applied to chick embryos in ovo, followed by incubation for 12 hr at 38°C with subsequent fixation.

Embryonic Surgeries

For the neural tube/DRG ablation, the left neural tube hemisphere and adjacent DRGs were removed entirely from the brachial to the first thoracic segments at HH22. For the dorsolateral skin epithelial-mesodermal ablation, the dorsolateral presumptive skin together with the underlying mesoderm and the dorsal part of the dermamyotome were removed from the brachial to the first thoracic segments at HH22. For the axotomization, spinal nerves of the brachial plexus were sectioned on the left side of HH27 embryos. A more detailed description is outlined in the Supplemental Data.

Nerve Transection in Adult Mice

The right sciatic nerves of eight 4-week-old Krox20^{YFP} mice were exposed and ligated at mid-thigh level with sterile suture silk, and the nerve was cut distally to the suture. Animals were sacrificed after 80 days. A more detailed description is outlined in the Supplemental Data.

DRG and Nerve Cultures

Chick embryos were transfected in ovo at HH13 with the GFP plasmid (1 μg/μl). HH29 DRGs and nerves were cultured in 24-well plates in melanocytic differentiation medium. See Supplemental Data for details.

Slice Tissue Cultures

Chick embryos were transfected in ovo at HH13 with the GFP plasmid (1 μg/μl) together with siRNA4 and siRNA42 (1.5 μg/μl each). Preparation of slice tissue cultures from HH24 and HH27 chick embryos followed the method of Lopez-Bendito et al. (Lopez-Bendito et al., 2006) adapted for chick embryos. Details are included in the Supplemental Data.

SUPPLEMENTAL DATA

Supplemental data include Supplemental Experimental Procedures, Supplemental References, and thirteen figures and can be found with this article online at http://www.cell.com/supplemental/S0092-8674(09)01043-5.

ACKNOWLEDGMENTS

We thank Michael Wegner, Vince Hearing, and Yoshio Wakamatsu for the generous gifts of antibodies directed against Sox10, Dct and MEBL-1, respectively. This work was supported by the Swedish Research Council, the Swedish Foundation for Strategic Research, Linné grants (CEDB and DBRM grants), the Swedish Cancer Foundation, Swedish Child Cancer Foundation, the Swedish Brain Foundation, Bertil Hållsten Research Foundation, EU FP7 MOLPARK collaborative project, and ERC advanced grant (232675) to P.E., and Knut and Alice Wallenberg Foundation (CLICK Imaging Facility). I.A. was supported by the Swedish Research Council. F.L. was supported by the Swedish Medical Research Council (K2007-77PK-20285-01-6) and the European Union (Marie Curie MEIF-CT-2006-039237). U.S. was supported by the Swiss National Science Foundation and the National Center for Competence in Research Neural Plasticity and Repair.

Received: July 1, 2008
Revised: April 3, 2009
Accepted: July 22, 2009
Published: October 15, 2009

REFERENCES

Aoki, Y., Saint-Germain, N., Gyda, M., Magner-Fink, E., Lee, Y.H., Credidio, C., and Saint-Jeannet, J.P. (2003). Sox10 regulates the development of neural crest-derived melanocytes in Xenopus. Dev. Biol. *259*, 19–33.

Bronner, M.E., and Cohen, A.M. (1979). Migratory patterns of cloned neural crest melanocytes injected into host chicken embryos. Proc. Natl. Acad. Sci. USA *76*, 1843–1847.

Dorris, F. (1938). The production of pigment in vitro by chick neural rest. Arch Entwicklungsmech Organ *138*, 323–334.

Dorris, F. (1939). The production of pigment by chick neural crest in grafts to the 3-day limb bud. J. Exp. Zool. *86*, 315–345.

Dorsky, R.I., Raible, D.W., and Moon, R.T. (2000). Direct regulation of nacre, a zebrafish MITF homolog required for pigment cell formation, by the Wnt pathway. Genes Dev. *14*, 158–162.

Dunn, K.J., Williams, B.O., Li, Y., and Pavan, W.J. (2000). Neural crest-directed gene transfer demonstrates Wnt1 role in melanocyte expansion and differentiation during mouse development. Proc. Natl. Acad. Sci. USA *97*, 10050–10055.

Dupin, E., Real, C., Glavieux-Pardanaud, C., Vaigot, P., and Le Douarin, N.M. (2003). Reversal of developmental restrictions in neural crest lineages: transition from Schwann cells to glial-melanocytic precursors in vitro. Proc. Natl. Acad. Sci. USA *100*, 5229–5233.

DuShane, G. (1935). An experimental study of the origin of pigment cells in amphibian. J. Exp. Zool. *72*, 1–31.

Erickson, C.A. (1993). From the crest to the periphery: control of pigment cell migration and lineage segregation. Pigment Cell Res. *6*, 336–347.

Fetsch, J.F., Michal, M., and Miettinen, M. (2000). Pigmented (melanotic) neurofibroma: a clinicopathologic and immunohistochemical analysis of 19 lesions from 17 patients. Am. J. Surg. Pathol. *24*, 331–343.

Fox, M.H. (1949). Analysis of some phases of melanoblast migration in the barred Plymouth Rock embryos. Physiol. Zool. *22*, 1–22.

Gambardella, L., Schneider-Maunoury, S., Voiculescu, O., Charnay, P., and Barrandon, Y. (2000). Pattern of expression of the transcription factor Krox-20 in mouse hair follicle. Mech. Dev. *96*, 215–218.

Gray, P.A., Fu, H., Luo, P., Zhao, Q., Yu, J., Ferrari, A., Tenzen, T., Yuk, D.I., Tsung, E.F., Cai, Z., et al. (2004). Mouse brain organization revealed through direct genome-scale TF expression analysis. Science *306*, 2255–2257.

Honore, S.M., Aybar, M.J., and Mayor, R. (2003). Sox10 is required for the early development of the prospective neural crest in Xenopus embryos. Dev. Biol. *260*, 79–96.

Huszar, D., Sharpe, A., Hashmi, S., Bouchard, B., Houghton, A., and Jaenisch, R. (1991). Generation of pigmented stripes in albino mice by retroviral marking of neural crest melanoblasts. Development *113*, 653–660.

Inomata, K., Aoto, T., Binh, N.T., Okamoto, N., Tanimura, S., Wakayama, T., Iseki, S., Hara, E., Masunaga, T., Shimitzu, H., and Nishimura, E.K. (2009). Genotoxic stress abrogates renewal of melanocyte stem cells by triggering their differentiation. Cell *137*, 1088–1099.

Jeffery, W.R., Strickler, A.G., and Yamamoto, Y. (2004). Migratory neural crest-like cells form body pigmentation in a urochordate embryo. Nature *431*, 696–699.

Jessen, K.R., and Mirsky, R. (2005). The origin and development of glial cells in peripheral nerves. Nat. Rev. Neurosci. *6*, 671–682.

Jin, E.J., Erickson, C.A., Takada, S., and Burrus, L.W. (2001). Wnt and BMP signaling govern lineage segregation of melanocytes in the avian embryo. Dev. Biol. *233*, 22–37.

Johnston, M.C. (1966). A radioautographic study of the migration and fate of cranial neural crest cells in the chick embryo. Anat. Rec. *156*, 143–155.

Le Douarin, N. (1973). A biological cell labeling technique and its use in expermental embryology. Dev. Biol. *30*, 217–222.

Lemke, G.E., and Brockes, J.P. (1984). Identification and purification of glial growth factor. J. Neurosci. *4*, 75–83.

Leone, D.P., Genoud, S., Atanasoski, S., Grausenburger, R., Berger, P., Metzger, D., Macklin, W.B., Chambon, P., and Suter, U. (2003). Tamoxifen-inducible glia-specific Cre mice for somatic mutagenesis in oligodendrocytes and Schwann cells. Mol. Cell. Neurosci. *22*, 430–440.

Lopez-Bendito, G., Cautinat, A., Sanchez, J.A., Bielle, F., Flames, N., Garratt, A.N., Talmage, D.A., Role, L.W., Charnay, P., Marin, O., and Garel, S. (2006). Tangential neuronal migration controls axon guidance: a role for neuregulin-1 in thalamocortical axon navigation. Cell *125*, 127–142.

Mackenzie, M.A., Jordan, S.A., Budd, P.S., and Jackson, I.J. (1997). Activation of the receptor tyrosine kinase Kit is required for the proliferation of melanoblasts in the mouse embryo. Dev. Biol. *192*, 99–107.

Marmigere, F., Montelius, A., Wegner, M., Groner, Y., Reichardt, L.F., and Ernfors, P. (2006). The Runx1/AML1 transcription factor selectively regulates development and survival of TrkA nociceptive sensory neurons. Nat. Neurosci. *9*, 180–187.

Marmigere, F., and Ernfors, P. (2007). Specification and connectivity of neuronal subtypes in the sensory lineage. Nat. Rev. Neurosci. *8*, 114–127.

Maro, G.S., Vermeren, M., Voiculescu, O., Melton, L., Cohen, J., Charnay, P., and Topilko, P. (2004). Neural crest boundary cap cells constitute a source of neuronal and glial cells of the PNS. Nat. Neurosci. *7*, 930–938.

Meier, C., Parmantier, E., Brennan, A., Mirsky, R., and Jessen, K.R. (1999). Developing Schwann cells acquire the ability to survive without axons by establishing an autocrine circuit involving insulin-like growth factor, neurotrophin-3, and platelet-derived growth factor-BB. J. Neurosci. *19*, 3847–3859.

Mintz, B. (1967). Gene control of mammalian pigmentary differentiation. I. Clonal origin of melanocytes. Proc. Natl. Acad. Sci. USA *58*, 344–351.

Montelius, A., Marmigere, F., Baudet, C., Aquino, J.B., Enerback, S., and Ernfors, P. (2007). Emergence of the sensory nervous system as defined by Foxs1 expression. Differentiation *75*, 404–417.

Nakagawa, S., and Takeichi, M. (1998). Neural crest emigration from the neural tube depends on regulated cadherin expression. Development *125*, 2963–2971.

Rawles, M. (1947). Origin of pigment cells from neural crest in the mouse embryo. Physiol. Zool. *20*, 248–270.

Riethmacher, D., Sonnenberg-Riethmacher, E., Brinkmann, V., Yamaai, T., Lewin, G.R., and Birchmeier, C. (1997). Severe neuropathies in mice with targeted mutations in the ErbB3 receptor. Nature *389*, 725–730.

Ris, H. (1941). An experimental study on the origin of melanophorese in birds. Physiol. Zool. *14*, 48–66.

Rizvi, T.A., Huang, Y., Sidani, A., Atit, R., Largaespada, D.A., Boissy, R.E., and Ratner, N. (2002). A novel cytokine pathway suppresses glial cell melanogenesis after injury to adult nerve. J. Neurosci. *22*, 9831–9840.

Serbedzija, G.N., Bronner-Fraser, M., and Fraser, S.E. (1989). A vital dye analysis of the timing and pathways of avian trunk neural crest cell migration. Development *106*, 809–816.

Serbedzija, G.N., Fraser, S.E., and Bronner-Fraser, M. (1990). Pathways of trunk neural crest cell migration in the mouse embryo as revealed by vital dye labelling. Development *108*, 605–612.

Steingrimsson, E., Copeland, N.G., and Jenkins, N.A. (2004). Melanocytes and the microphthalmia transcription factor network. Annu. Rev. Genet. *38*, 365–411.

Stewart, H.J., Morgan, L., Jessen, K.R., and Mirsky, R. (1993). Changes in DNA synthesis rate in the Schwann cell lineage in vivo are correlated with the precursor–Schwann cell transition and myelination. Eur. J. Neurosci. *5*, 1136–1144.

Thomas, A.J., and Erickson, C.A. (2008). The making of a melanocyte: the specification of melanoblasts from the neural crest. Pigment Cell Melanoma Res *21*, 598–610.

Topilko, P., Schneider-Maunoury, S., Levi, G., Baron-Van Evercooren, A., Chennoufi, A.B., Seitanidou, T., Babinet, C., and Charnay, P. (1994). Krox-20 controls myelination in the peripheral nervous system. Nature *371*, 796–799.

Twitty, V. (1936). Correlated genetic and embryological experiments on triturus. I and II. J. Exp. Zool. *74*, 239–302.

Weinreb, I., Labonte, S., Goli, H., Chetty, R., and Ghazarian, D. (2007). Cutaneous melanocytoneuroma: the first case of a distinctive intraneural tumor with dual nerve sheath and melanocytic differentiation. J. Cutan. Pathol. *34* (*Suppl 1*), 52–57.

Weston, J.A. (1963). A radioautographic analysis of the migration and localization of trunk neural crest cells in the chick. Dev. Biol. *6*, 279–310.

Wilkie, A.L., Jordan, S.A., and Jackson, I.J. (2002). Neural crest progenitors of the melanocyte lineage: coat colour patterns revisited. Development *129*, 3349–3357.

Voiculescu, O., Charnay, P., and Schneider-Maunoury, S. (2000). Expression pattern of a Krox-20/Cre knock-in allele in the developing hindbrain, bones, and peripheral nervous system. Genesis *26*, 123–126.

Zirlinger, M., Lo, L., McMahon, J., McMahon, A.P., and Anderson, D.J. (2002). Transient expression of the bHLH factor neurogenin-2 marks a subpopulation of neural crest cells biased for a sensory but not a neuronal fate. Proc. Natl. Acad. Sci. USA *99*, 8084–8089.